Front. Optoelectron. 2016, 9(3): 362–376
DOI 10.1007/s12200-016-0553-z

REVIEW ARTICLE

Linear all-optical signal processing using silicon micro-ring resonators

Yunhong DING (✉)[1], Haiyan OU[1], Jing XU[2], Meng XIONG[1], Yi AN[1], Hao HU[1], Michael GALILI[1], Abel Lorences RIESGO (✉)[3], Jorge SEOANE[1], Kresten YVIND[1], Leif Katsuo OXENLØWE[1], Xinliang ZHANG[2], Dexiu HUANG (✉)[2], Christophe PEUCHERET (✉)[4]

1 Department of Photonics Engineering, Technical University of Denmark, 2800 Kgs. Lyngby, Denmark
2 Wuhan National Laboratory for Optoelectronics, Huazhong University of Science and Technology, Wuhan 430074, China
3 Department of Microtechnology and Nanoscience, Chalmers University of Technology, Gothenburg, Sweden
4 FOTON Laboratory, CNRS UMR 6082, University of Rennes 1, ENSSAT, 22300 Lannion, France

© Higher Education Press and Springer-Verlag Berlin Heidelberg 2016

Abstract Silicon micro-ring resonators (MRRs) are compact and versatile devices whose periodic frequency response can be exploited for a wide range of applications. In this paper, we review our recent work on linear all-optical signal processing applications using silicon MRRs as passive filters. We focus on applications such as modulation format conversion, differential phase-shift keying (DPSK) demodulation, modulation speed enhancement of directly modulated lasers (DMLs), and monocycle pulse generation. The possibility to implement polarization diversity circuits, which reduce the polarization dependence of standard silicon MRRs, is illustrated on the particular example of DPSK demodulation.

Keywords linear all-optical signal processing, micro-ring resonator (MRR), polarization diversity, silicon-on-insulator (SOI)

1 Introduction

All-optical signal processing consists in manipulating the properties of light waves carrying information signals without resorting to electronic means following photodetection. This includes the implementation of functionalities such as signal temporal or spectral conditioning, wavelength conversion, regeneration, switching, modulation format conversion, clock recovery, etc. Generally, the purpose of all-optical signal processing is to avoid electronic bottlenecks by performing the required functionalities directly on optical high-speed modulated signals or by processing a number of (typically wavelength-multiplexed) channels in parallel, thereby overcoming the speed limitation of electronics, or providing cost savings.

Typically, all-optical signal processing functionalities are demonstrated using nonlinear interactions in a wide range of materials and devices, including the use of highly nonlinear optical fibers [1]), nonlinear waveguides (e.g., silicon [2] or chalcogenide [3]), semiconductor optical amplifiers (SOAs) [4], periodically-poled lithium niobate (PPLN) [5], etc. However, some functionalities can also be realized linearly by appropriate filtering of the signal.

In this paper, we show how silicon micro-ring resonators (MRRs) [6] can be used to implement a variety of signal processing functionalities, including multi-channel and ultra-high speed modulation format conversion, multi-channel demodulation of phase modulated signals, signal conditioning and waveform generation. Silicon MRRs present a number of advantages. Their periodic transfer functions can be used for the parallel processing of several wavelength channels, while transfer function engineering enables flexible tailoring of the signal properties. The devices are compact and can be manufactured with potentially low-cost and high yield using well-controlled micro-electronics fabrication processes. The compactness of the devices means that they have potential for applications in telecommunication, data-communication, as well as on-chip communication. For applications where the signal to be processed has been propagating over a length of optical fiber, the inherent polarization sensitivity of silicon waveguides appears first as a limitation.

Received September 18, 2015; accepted January 8, 2016

E-mails: yudin@fotonik.dtu.dk, lorences@chalmers.se, wnlo2@mail.hust.edu.cn, christophe.peucheret@univ-rennes1.fr

However, we also show in this work that devices with reduced polarization sensitivity can be designed and fabricated on the silicon platform, thereby allowing the demonstration of polarization- independent linear signal processing.

This paper is structured as follows. An introduction to silicon MRRs and their fabrication is provided in Section 2. In Section 3, the use of a single MRR to perform modulation format conversion from the return-to-zero (RZ) to the non return-to-zero (NRZ) modulation format is demonstrated for both on-off keying (OOK) and phase-shift keying (PSK) signals at 40 Gbit/s, as well as for ultra-high speed optical time division multiplexed (OTDM) signals, resulting in the first demonstration of NRZ signal generation at an unprecedented bit rate of 640 Gbit/s. Section 4 deals with the demodulation of differential PSK (DPSK) signals. In Section 5, it is shown how filtering of the adiabatically chirped signal generated from a directly modulated laser (DML) by an MRR can enable such a laser to be operated at a higher bit rate than what is expected from its nominal bandwidth. An add-drop MRR with adjustable coupling coefficients can be used to synthesize an ultra-wide band (UWB) signal, as demonstrated in Section 6. The implementation of linear signal processing with reduced polarization sensitivity thanks to the use of a polarization diversity circuit is described in Section 7. The results are finally summarized in Section 8.

2 Silicon MRRs

MRRs are very attractive devices for integration [7,8] thanks to their property of supporting traveling wave resonance modes without any reflective facet. Thanks to this great advantage, MRR-based laser sources [9], electro-optical modulators [10], optical memory units [11–13], optical bandpass filters [14], etc., have been widely investigated. The through and drop transfer functions of a standard add/drop MRR, as shown in Fig. 1, can be expressed as [15]

$$t_{\text{through}} = \frac{r_1 - ar_2\exp(-\mathrm{j}\theta)}{1 - ar_1r_2\exp(-\mathrm{j}\theta)}, \tag{1}$$

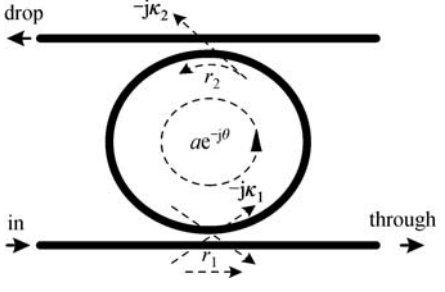

Fig. 1 Schematic of a standard add-drop micro-ring resonator

$$t_{\text{drop}} = \frac{\kappa_1\kappa_2\sqrt{a\exp(-\mathrm{j}\theta)}}{1 - ar_1r_2\exp(-\mathrm{j}\theta)}, \tag{2}$$

where r_i and κ_i are the field transmission and coupling coefficients, respectively, of the coupling regions of the resonator, satisfying the relation $r_i^2 + \kappa_i^2 = 1$ for lossless coupling with $i = 1$ and 2 denoting the through and drop coupling regions, respectively. θ and a are the roundtrip phase shift and field transmission coefficients along the ring waveguide, respectively. If the drop coupling coefficient κ_2 equals to zero, the MRR is degraded to all-pass type. The free spectral range (FSR) $\Delta\lambda_{\text{FSR}}$ of a MRR can be expressed as [16]

$$\Delta\lambda_{\text{FSR}} = \frac{\lambda^2}{n_{\text{g}}L}, \tag{3}$$

where n_{g} is the group index, and L is the roundtrip length. The Q value of an add/drop MRR, which is a measure of the sharpness of the resonance relative to its central frequency, can be further expressed as [16]

$$Q = \frac{\lambda_0}{\Delta\lambda_{\text{FWHM}}} \approx \frac{\pi\lambda_0}{\Delta\lambda_{\text{FSR}}}\frac{\sqrt{ar_1r_2}}{1 - ar_1r_2}, \tag{4}$$

where λ_0 is the resonance wavelength, $\Delta\lambda_{\text{FWHM}}$ is the 3-dB resonance bandwidth of the drop transmission. In Eq. (4), weak coupling is assumed for both through and drop coupling regions. An important feature of MRRs is that their FSR can be easily controlled by designing the size of the micro-ring, and resonance bandwidth or equivalently Q value can be easily engineered by controlling the coupling coefficients of the coupling regions, allowing MRRs to be optimized for wavelength division multiplexing (WDM) linear all-optical signal processing applications.

Silicon-on-insulator (SOI) is considered to be one of the most promising platforms for integrated optical devices thanks to its complementary metal-oxide-semiconductor (CMOS) compatible fabrication process. Moreover, the ultra-high refractive index contrast between silicon (n≈3.5) and buried oxide (BOX) layers (n≈1.45) enables the realization of compact SOI devices. In the following work, the silicon devices have been fabricated by standard electron beam (e-beam) lithography-based nano-fabrication processes, as shown in Fig. 2. First, a thin layer of e-beam resist (ZEP520A) is spin coated on the SOI sample. The structures are then defined by e-beam writing (JEOL JBX-9300FS) and subsequent developing. After that, the sample is etched by inductively coupled plasma reactive ion etching (ICP-RIE) to transfer the patterns to the top silicon layer. The final device is obtained by stripping the residual e-beam resist after ICP etching.

3 Modulation format conversion

Optical modulation format conversion is a potentially

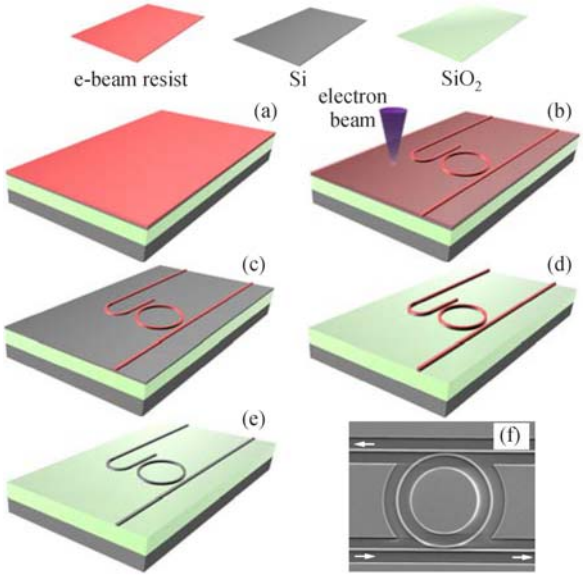

Fig. 2 Fabrication process of a standard silicon micro-ring resonator (MRR). (a) E-beam resist spinning; (b) e-beam exposure; (c) developing; (d) ICP etching; (e) e-beam resist stripping; (f) scanning electron microscope (SEM) picture of a typical fabricated add/drop MRR

important functionality in nodes interfacing optical networks operating with different modulation formats. Format conversion between RZ and NRZ formats is one essential conversion, since both formats are widely used in different parts of optical networks [17]. A good modulation format converter requires low power consumption and the ability to support simultaneous multiple channel operation to accommodate widely deployed WDM networks. The use of passive filters such as optical nano-fiber ring resonators [18] and fiber delay-interferometers (DIs) [17] has been demonstrated for single and multiple channels RZ-to-NRZ format conversion. However, both fiber DIs and nano-fiber ring resonators require stabilization, and integrated implementations would be preferred.

3.1 WDM RZ-OOK to NRZ-OOK format conversion

Thanks to the periodic property of the MRR transmission, a single silicon MRR is able to perform multi-channel RZ-OOK to NRZ-OOK format conversion based on optical spectrum transformation [19], which consists in transforming an RZ spectrum to an NRZ-like spectrum by optical filtering. The corresponding experimental setup is presented in Fig. 3. Four channels of continuous wave (CW) laser light with wavelengths of 1548.16, 1549.76, 1551.36, and 1552.97 nm (200-GHz channel spacing) are combined in a coupler, amplified by an erbium-doped fiber amplifier (EDFA), and simultaneously modulated at 50 Gbit/s in the 33% RZ-OOK format in two Mach-Zehnder modulators (MZMs). The four modulated RZ channels are amplified using a second EDFA and further de-correlated by 50 m dispersion-compensating fiber (DCF). A set of polarization controllers (PCs) followed by a polarizer (Pol.) and a second PC are used to align the input polarization of all WDM channels to the transverse electric (TE) mode of the waveguide. The WDM RZ signal is then converted to a WDM NRZ signal by the MRR. Finally, the amplified converted WDM NRZ signal is wavelength demultiplexed by an arrayed waveguide grating (AWG) with 3-dB bandwidth of 62 GHz, and detected in a pre-amplified receiver.

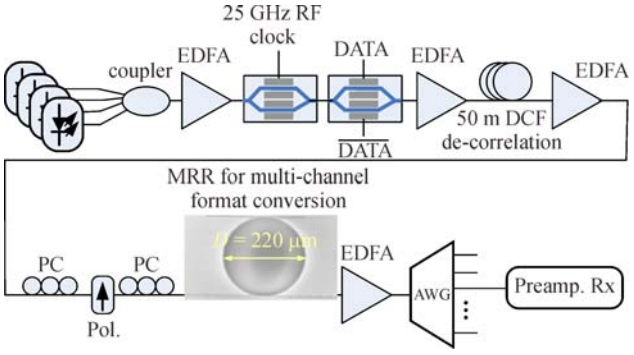

Fig. 3 Experimental setup for multiple WDM channels RZ-OOK to NRZ-OOK format conversion

Figure 4 shows the measurement results. The MRR has an FSR of 100 GHz and an optimized Q value of 7900 with an extinction ratio (ER) as high as 20 dB, as shown in Fig. 4(a). The first order harmonic components in the spectra of all four RZ channels are suppressed simultaneously by the MRR, resulting in an effective spectrum transformation from WDM RZ to WDM NRZ, as illustrated in Figs. 4(a) and 4(b). Accordingly, the RZ eye-diagram (see Fig. 4(c)) is effectively converted to a very clear NRZ format eye-diagram (see Fig. 4(d)), which is very close to the reference electrically modulated NRZ signal (see Fig. 4(e)). Figure 4 (f) shows the result of bit error ratio (BER) measurements with a 2^7–1 pseudorandom binary sequence (PRBS). BER values below 10^{-9} are obtained for all the four converted NRZ channels with limited power penalty with respect to the reference electrically modulated NRZ signal. The moderate power penalty is introduced by inter-channel crosstalk. It should be mentioned that, for this particular application, the channel spacing should be a multiple of the FSR of the MRR, which is dictated by the spacing between the discrete tones in the spectrum of the RZ signal, hence its bit rate.

3.2 Simultaneous RZ-OOK to NRZ-OOK and RZ-DPSK to NRZ-DPSK format conversion

Apart from OOK modulation, the use of an MRR for format conversion is also compatible with DPSK modulation, allowing simultaneous RZ-OOK to NRZ-OOK and

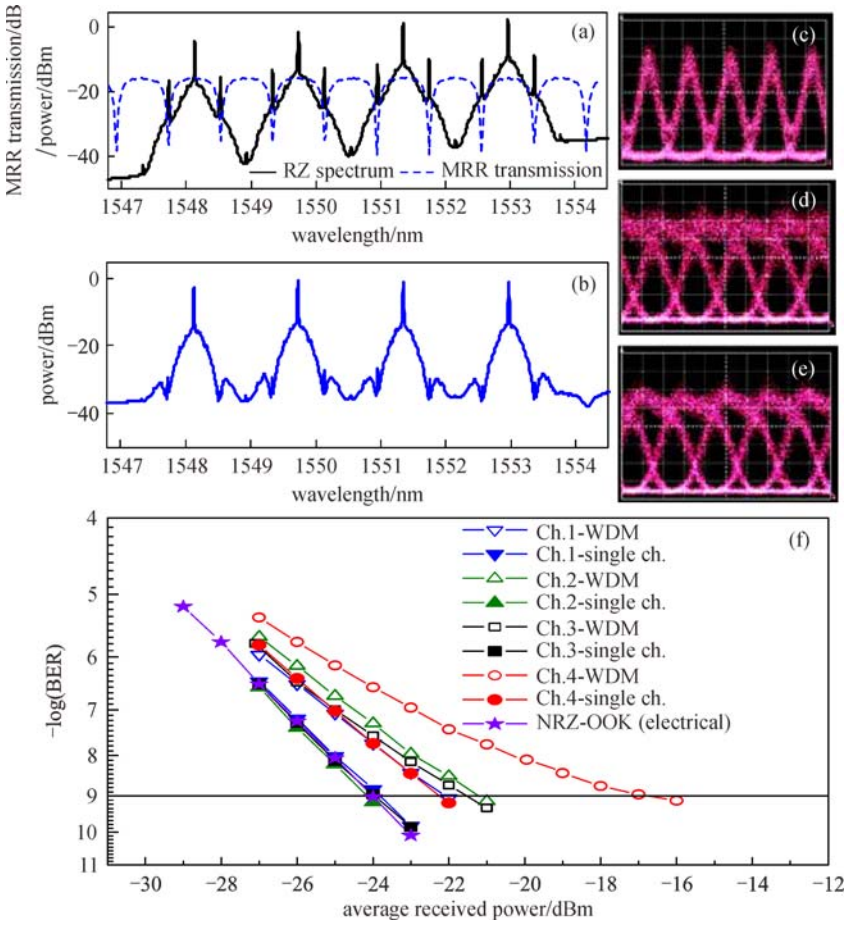

Fig. 4 (a) WDM RZ signal spectrum and MRR through transmission; (b) converted WDM NRZ signal spectrum; measured eye-diagrams of (c) single RZ signal, (d) converted NRZ signals and (e) original reference NRZ signal; (f) BER measurements of the converted NRZ channels in single-channel and WDM operation, as well as an electrically generated reference NRZ signal

RZ-DPSK to NRZ-DPSK format conversion by a single MRR [20]. The experimental setup for simultaneous RZ-to-NRZ format conversion of OOK and DPSK is shown in Fig. 5. Two CW lights at 1549.35 and 1551.36 nm are modulated at 41.6 Gbit/s in the 33% RZ-DPSK and 33% RZ-OOK format, respectively, by two sets of two MZMs. The PRBS length is 2^{31}–1 for both channels. The OOK and DPSK signals are then combined in a 3-dB coupler and amplified by an EDFA. A set of PC-Pol.-PC is used afterwards to adjust the states of polarization of the signals to the transverse magnetic (TM) mode of the MRR. The converted NRZ-OOK and NRZ-DPSK signals after the MRR are filtered by an optical bandpass filter (OBPF) and finally detected in a pre-amplified receiver. A 1-bit fiber DI followed by balanced detection in a pair of 45-GHz photodiodes is used in the DPSK receiver, while the OOK signal is detected using a single 45-GHz photodiode.

The fabricated MRR has an FSR of 83 GHz, a Q value of 5200, and an ER of 25 dB, as shown in Fig. 6(a). The spectra transformation is also shown. Since the central

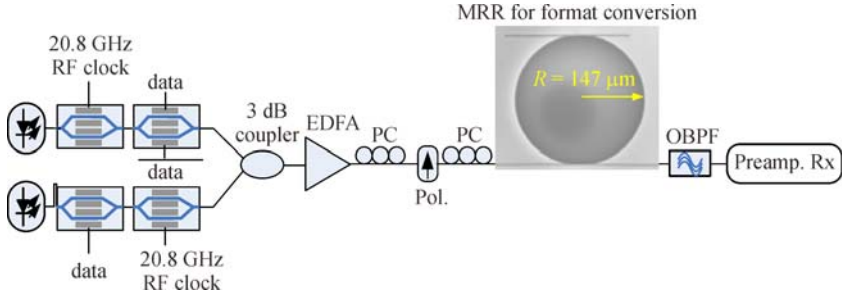

Fig. 5 Experimental setup for simultaneous RZ-OOK to NRZ-OOK and RZ-DPSK to NRZ-DPSK format conversion

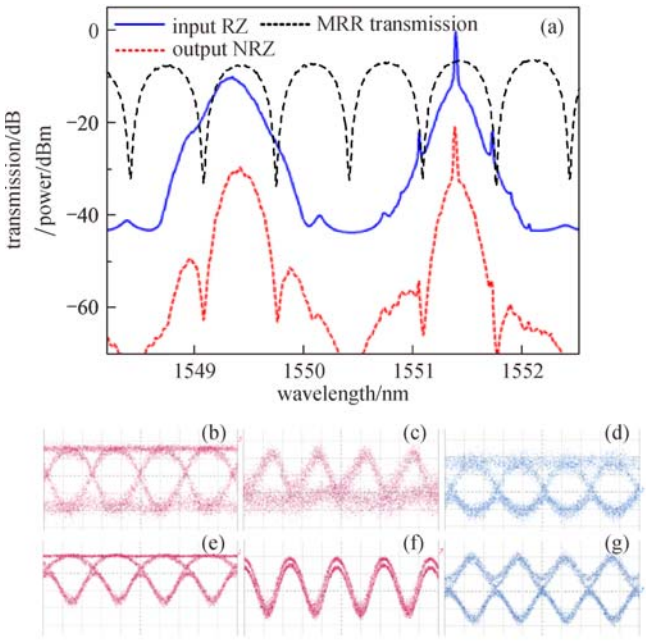

Fig. 6 (a) MRR through transmission and spectra of the two-channel input RZ signals and the converted NRZ signals; measured eye-diagrams of (b) input RZ-OOK (single channel), (c) input RZ-DPSK (single channel), (d) demo-dulated signal of the input RZ-DPSK after balanced detection, (e) converted NRZ-OOK (two-channel), (f) converted NRZ-DPSK (two-channel) and (g) demodulated signal of the converted NRZ-DPSK after balanced detection

wavelengths of the two input RZ signals are tuned to the centers between two notches of the MRR through transmission, specific spectral components of both RZ-OOK and RZ-DPSK signals are effectively suppressed after the MRR and their spectra are successfully transformed to the spectra of NRZ signals. Accordingly, the eye-diagrams of RZ-OOK (see Fig. 6(b)) and RZ-DPSK (see Fig. 6(c)) are effectively converted to NRZ-OOK (see Fig. 6(e)) and NRZ-DPSK (see Fig. 6(f)) eye-diagrams, simultaneously. Figure 7 shows the results of BER measurements for both single channel and simultaneous two-channel format conversion. It can be seen that BER values below 10^{-9} can be obtained for both OOK and DPSK channels after format conversion. In addition, there is nearly no cross talk between the two channels.

3.3 OTDM format conversion

OTDM is an essential multiplexing technique potentially allowing symbol rates beyond the limits currently achievable by electronic multiplexing [21]. OTDM makes use of RZ modulated signals with small duty cycles allowing temporal interleaving of the channels. However, traditional OTDM signal demultiplexing using an optical gate is very sensitive to timing jitter because of the fairly narrow pulse widths involved. Furthermore, OTDM signals are extremely sensitive to dispersion due to their broad spectra.

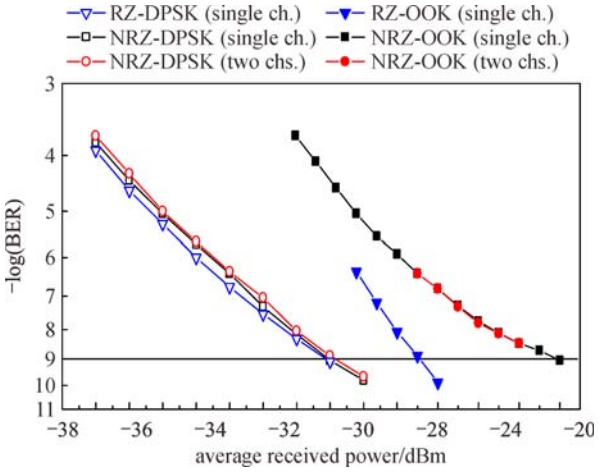

Fig. 7 BER measurements for input RZ-OOK, converted NRZ-OOK, input RZ-DPSK, and converted NRZ-DPSK for both single and two-channel operations

Being able to generate ultra-high speed signals modulated in the NRZ format would alleviate those issues, resulting in increased timing jitter tolerance in the demultiplexing process thanks to their flat top, as well as better resilience to dispersion and enhanced spectral efficiency [22]. Ultra-high speed NRZ signals can be generated using conventional OTDM techniques followed by all-optical modulation format conversion from RZ to NRZ, which can be performed in a silicon MRR [23].

Figure 8 shows the experimental setup for 640-Gbit/s NRZ signal generation. A 640-Gbit/s RZ OTDM signal with 2^7–1 PRBS at 1560 nm is first wavelength converted using a Kerr switch with an amplified CW probe at 1535.6 nm in a 200-m highly-nonlinear fiber (HNLF), resulting in the generation of a 640-Gbit/s pulse-to-pulse coherent RZ signal. This phase coherence ensures that the spectrum of the RZ signal contains discrete lines at frequencies that are multiple of the symbol rate, in contrast with the original OTDM signal where this phase coherence is lost in the time-multiplexing process. The converted RZ signal is then amplified and input to a silicon MRR in the TM mode in order to perform format conversion. The MRR has an FSR of 1280 GHz and Q value of 638. An OBPF is then used to reduce the amplitude ripples of the converted NRZ signal. Finally, the 640-Gbit/s NRZ OTDM signal is time-demultiplexed in a nonlinear optical loop mirror (NOLM) [24] before being detected in a 10-Gbit/s receiver.

Figure 9(a) illustrates the spectrum transformation of the 640-Gbit/s NRZ signal generation. As anticipated, the original 640-Gbit/s OTDM spectrum (blue) does not contain strong harmonic components at multiples of frequencies corresponding to the bit rate due to the lack of pulse-to-pulse phase coherence between the OTDM tributary channels. However, the 640-Gbit/s wavelength converted RZ spectrum (purple) displays clear and strong harmonic components, which are aligned with the notches of the MRR through transmission (dashed black) in order

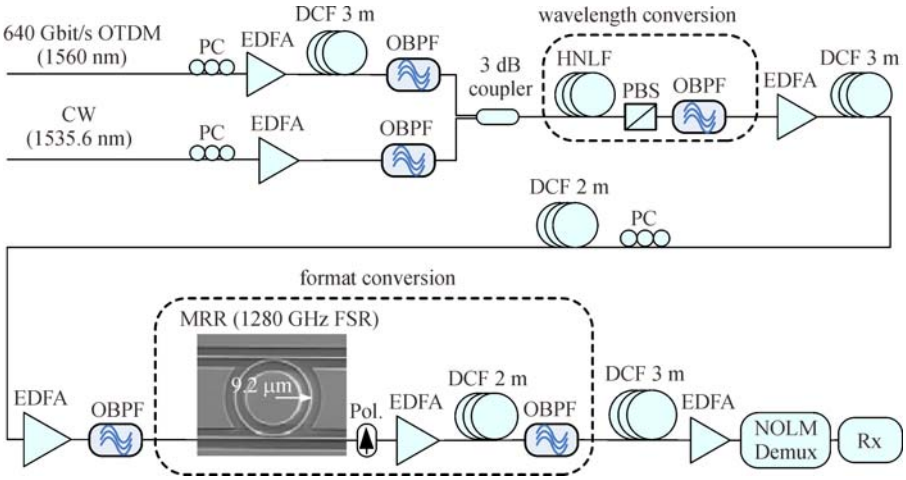

Fig. 8 Experimental setup for 640-Gbit/s RZ-to-NRZ format conversion

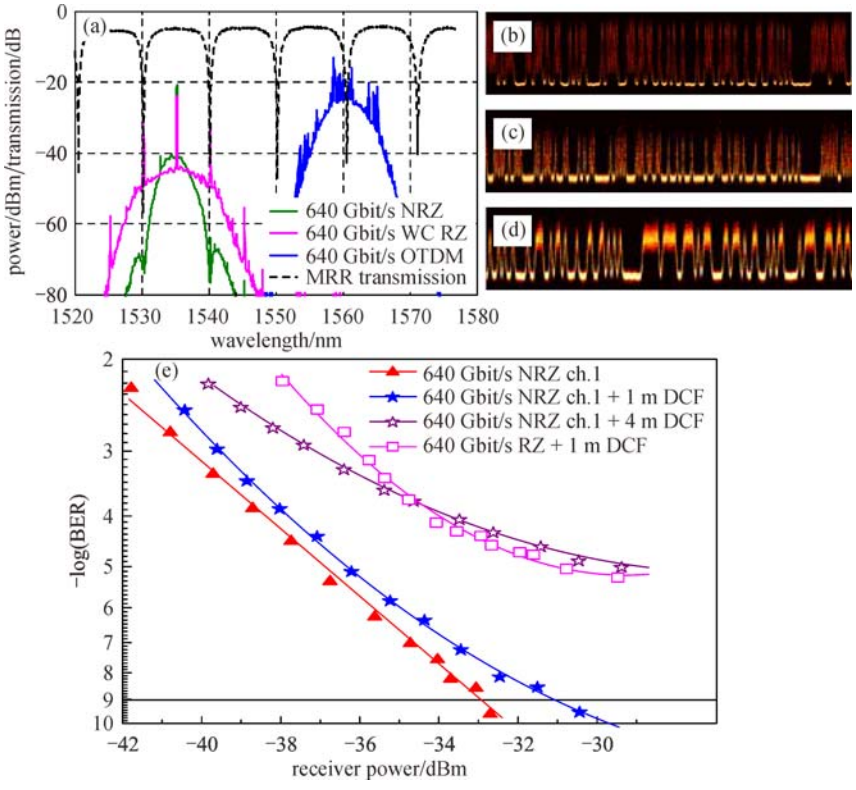

Fig. 9 (a) Spectra of the original OTDM (blue), wavelength converted RZ (purple), and format converted NRZ signals (green), as well as through transmission of the silicon MRR (dashed black); (b)–(d) optical sampling oscilloscope traces of the original incoherent 640-Gbit/s OTDM signal, 640-Gbit/s wavelength converted RZ signal, and the 640-Gbit/s format converted NRZ signal, respectively; (e) BER results with PRBS length of 2^7–1 for channel 1 demultiplexed from 640-Gbit/s NRZ with 1 and 4 m DCFs, and a demultiplexed tributary from the 640-Gbit/s wavelength converted RZ signal with 1 m DCF

to perform format conversion. After the OBPF, a 640-Gbit/s NRZ spectrum (green) is obtained, showing a much reduced bandwidth compared to the 640-Gbit/s wavelength converted RZ spectrum. To test the dispersion tolerance, short pieces of DCFs are added before demultiplexing the 640-Gbit/s NRZ and wavelength-converted RZ signals. BER measurement results are shown in Fig. 9(e). Good BER performance with power penalty as low as ~1.5 dB is obtained for the tributary demultiplexed from the 640-Gbit/s NRZ signal after 1-m DCF transmission. However, for the same DCF length, an error floor is present in the case of the 640-Gbit/s wavelength converted RZ signal. A similar error floor appears for the 640-Gbit/s NRZ signal after transmission

over 4 m DCF. Hence, it is clear that the 640-Gbit/s NRZ signal exhibits improved dispersion tolerance compared to the wavelength converted RZ signal.

4 DPSK demodulation

DPSK is a promising modulation format for optical communication networks. Compared to OOK, DPSK exhibits a 3-dB improvement in receiver sensitivity when balanced detection is employed, and is more tolerant to fiber nonlinearities [25]. Mach–Zehnder delay interferometers (MZDIs) [26] with 1-bit delay are typically used to demodulate DPSK signals. The use of silicon MRRs as DPSK demodulators has been recently proposed [27] and demonstrated [28] for single channel operation. Thanks to the periodic property of MRRs transfer functions, this scheme is also promising for multi-channel applications [29]. The experimental setup is shown in Fig. 10. Four channels of CW laser light with wavelengths of 1548.65, 1550.26, 1551.90, and 1553.54 nm (channel spacing of ~200 GHz) are combined in a coupler, amplified by an EDFA, then simultaneously modulated with a PRBS length of 2^{31}–1 at 40 Gbit/s in the NRZ-DPSK format in a MZM. The WDM NRZ-DPSK channels are then amplified by another EDFA and de-correlated in 150-m DCF. A set of PC-Pol.-PC is then used to align the input polarization of all channels to the TM mode of the silicon waveguide. Demodulated AMI and DB signals will be obtained at the through and drop ports of the MRR, respectively. Afterwards, 1-km standard single mode fiber (SSMF) is used to compensate the dispersion introduced by the DCF. The WDM demodulated signal is amplified by another EDFA, de-multiplexed by an AWG and finally detected in a pre-amplified receiver.

Figure 11 shows the measured MRR through and drop transmissions, and the spectra of the WDM NRZ-DPSK signals, as well as of the WDM AMI and DB signals demodulated by the MRR. The ER of the through transmission of the MRR is as high as 25 dB, its measured

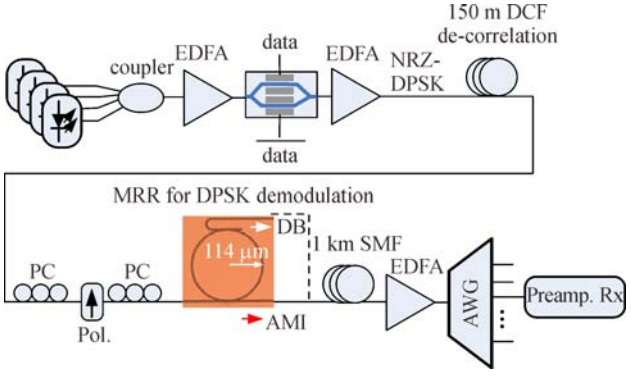

Fig. 10 Experimental setup for MRR based WDM NRZ-DPSK demodulation

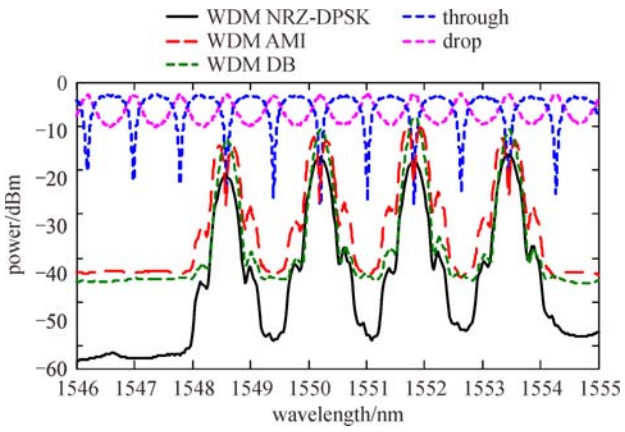

Fig. 11 Measured transfer functions for the TM mode at the through and drop ports of the fabricated MRR, and measured spectra of the WDM NRZ-DPSK signals, as well as of the WDM AMI and DB signals demodulated in a single MRR

FSR is 0.8 nm, corresponding to 100 GHz, and its Q value is 6700. The notches of the through transfer function and the peaks of the drop transfer function of the MRR are aligned to the carrier wavelengths of all the WDM channels, resulting in simultaneous demodulation of all channels to the AMI and DB formats, respectively. Figure 12 presents BER measurements for all channels at the output of the through (AMI) and drop (DB) ports. The inset pictures illustrate very clear eye-diagrams for the demodulated AMI and DB signals. For comparison purpose, the MRR is also substituted with a commercial fiber MZDI with 42.7-GHz FSR used for single channel demodulation. Although the BER for both through and drop port demodulations are worse than that of the MZDI, all the four channels reach bit error rates below 10^{-9}, without noticeable error floor. In addition, the optimized Q

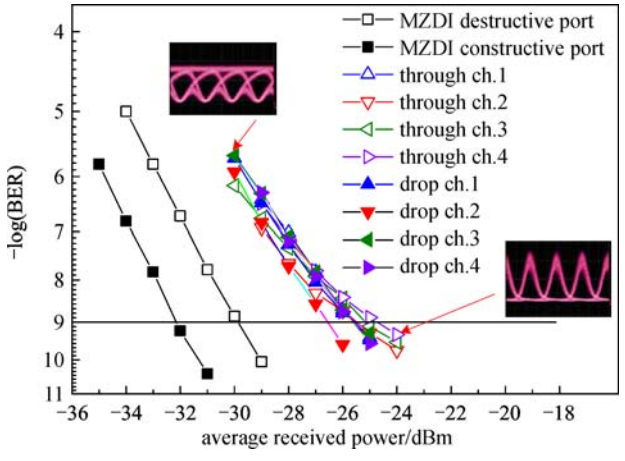

Fig. 12 BER measurements for the multiple channel AMI and DB signals demodulated by the MRR, as well as a single channel AMI and DB signal demodulated by the MZDI. The insets show typical eye-diagrams for the AMI and DB signals demodulated by the MRR

value of the MRR leads to similar receiver sensitivities for both through and drop port demodulations.

5 Modulation speed enhancement

An MRR can be used in order to enhance the modulation speed of a DML, as illustrated in Fig. 13. The operation bears some analogy with the principle of chirped managed lasers (CMLs), which consist of a DML biased at a high current with respect to the threshold, followed by an optical spectrum reshaping (OSR) filter [30]. Under these conditions, the laser is operated with a wide bandwidth, however at the expense of a limited ER, and its frequency chirp is dominated by its adiabatic contribution. By using the MRR through transmission to suppress the frequency components corresponding to the modulated zeros, both ER and eye-opening of the signal emitted by a DML operated beyond its nominal bit rate can be greatly improved [31].

This concept has been experimentally demonstrated using a commercially available 10-Gbit/s DFB laser modulated at 40 Gbit/s and a discrete custom-made silicon MRR with FSR of 200 GHz and Q value of 3300. The DML was thermally tuned to the short wavelength side of an MRR resonance (detuning of ~0.17 nm), as shown in Fig. 14(a). The MRR resonance was then used to filter the longer wavelength side of the signal spectrum, which corresponds to the emitted zeros. As a result, the eye-diagram at the output of the DML is significantly opened thanks to the MRR and the zero level is largely suppressed, at the expense of some overshoot on the one level. Figure 14(b) shows the BER performance of the signal emitted at 40 Gbit/s by the DML and that of the signal filtered by the MRR, directly after the resonator as well as after different lengths of SSMF. The BER improvement due to the MRR filtering is evident. The sensitivity at 10^{-9} of the filtered signal was about −17.2 dBm whereas an error-floor of 1.2×10^{-6} was obtained for an average input power of −9 dBm for the DML signal without MRR filtering. The filtered signal could furthermore be transmitted over SSMF lengths compatible with short reach applications, with a power penalty of about 1.5 dB after 3 km and a signal still detected error-free after 4.5 km uncompensated SSMF. Such a scheme has also been shown to be directly applicable to vertical cavity surface-emitting lasers (VCSELs) [32], and is promising for the development of compact high-speed sources for short-reach systems.

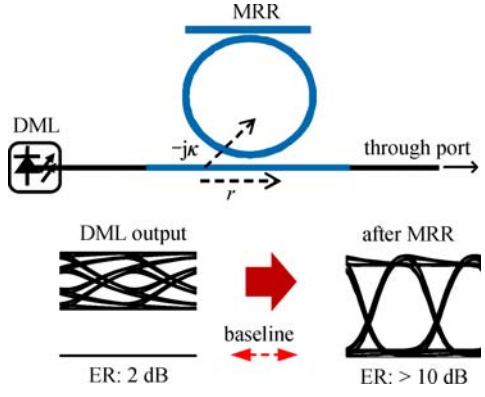

Fig. 13 Principle of using an MRR for modulation speed enhancement. The method is illustrated with simulated waveforms and eye-diagrams corresponding to a 10-Gbit/s DML driven with a 42.8-Gbit/s signal

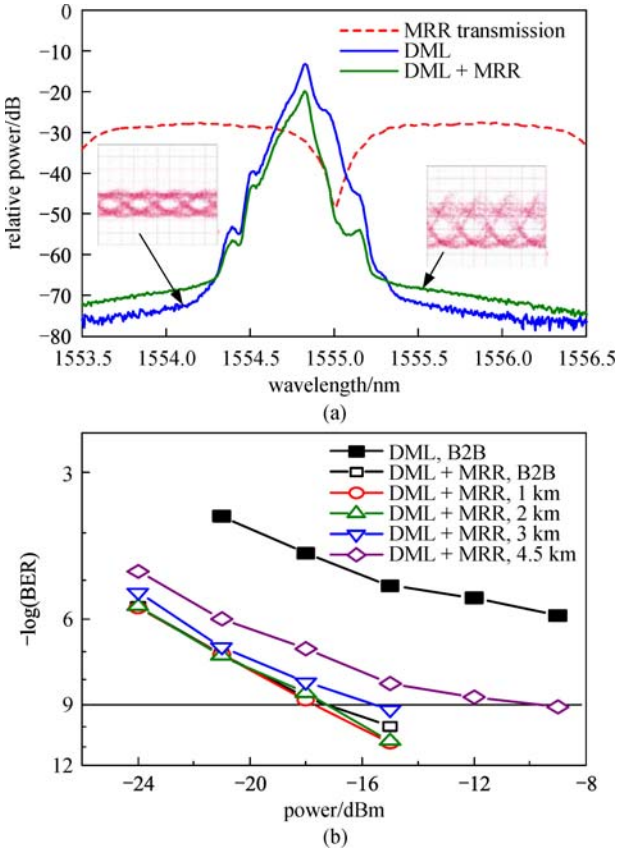

Fig. 14 (a) MRR through transmission and spectra of a 10-Gbit/s DML operated at 40 Gbit/s before and after the MRR. The insets show the eye diagrams measured directly at the DML output and after filtering by the MRR; (b) BER performance at the DML output (DML, B2B), after the MRR (DML + MRR, B2B), as well as after different lengths of SSMF

6 Monocycle pulse synthesis

The photonic generation and distribution of UWB signals has been a very active area of research for high data rate wireless applications [33]. Thanks to their compact sizes, MRRs have been investigated for UWB monocycle signal generation using differentiation of a signal whose phase has been modulated by a Gaussian electrical signal by

phase-to-intensity conversion using the slope of the MRR transfer function [34]. In this context, an MRR resonance is traditionally offset related to the carrier wavelength of the phase modulated optical signal. As a consequence, the slope of the MRR transmission performs PM-to-IM conversion of the Gaussian phase modulated optical signal. However, such a scheme relies on the generation of Gaussian electrical pulses, which may not be available from conventional electronic circuits. In contrast, it has been found that UWB monocycle signals can also be synthesized from standard NRZ electronics using an NRZ-DPSK signal generated in a Mach-Zehnder modulator filtered by a single MRR whose resonance is tuned to the carrier wavelength of the optical signal, provided that the MRR through and drop coupling coefficients are properly set [35]. The principle of the method is depicted schematically in Fig. 15(a). A CW laser is modulated in the NRZ-DPSK format in a MZM. The modulation results in intensity dips each time the phase of the signal is flipped between 0 and π. The modulated signal is then input to a silicon MRR in add-drop configuration (therefore with two coupling regions). By adjusting the values of the coupling coefficients of the through and drop ports (κ_1 and κ_2, respectively), a balanced monocycle signal can be obtained. Figure 15(b) represents the combination of values of κ_1^2 and κ_2^2 for which $A_1 = A_2$ for three signal rise times of 50, 100 and 200 ps. It can be seen that, for each value of the rise time of the phase modulating signal, two sets of (κ_1^2, κ_2^2) parameters that equalize A_1 and A_2 can be found. Each set corresponds to a given polarity of the monocycle pulse, as illustrated in Fig. 15(b). Consequently, the optimization of the UWB waveform requires MRRs with tunable coupling coefficients.

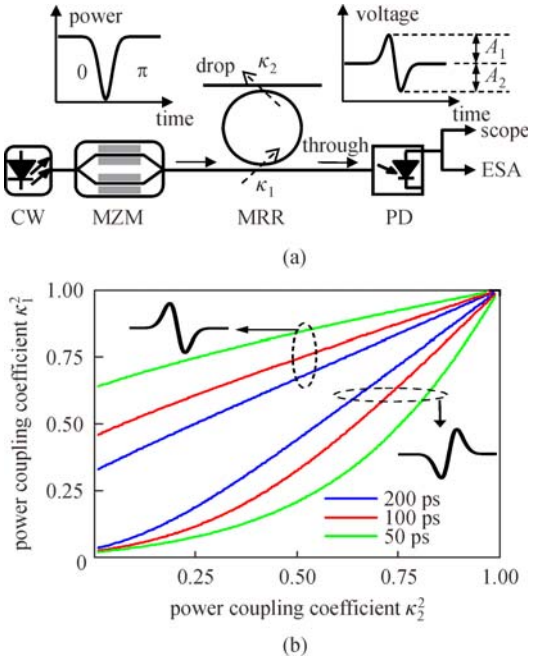

Fig. 15 (a) Principle of the UWB generation method; (b) calculated values of the MRR through and drop power coupling coefficients κ_1^2 and κ_2^2 resulting in monocycle pulses fulfilling the condition $A_1 = A_2$ for three electrical driving signal rise times of 50, 100 and 200 ps

To test this new concept, a silicon MRR with adjustable through and drop power coupling coefficients was designed and fabricated. The tunability of the coupling coefficients is achieved by two MZI structures which act as through and drop couplers, as shown in Fig. 16. Thermal tuning enables to control the relative phase shifts between the two arms of each MZI, and consequently the power coupling ratio between the ring and the input and drop waveguides. The device operates in the TM mode with an FSR of 100 GHz. The fabricated device was used in an UWB generation experiment at 625-Mbit/s. The experimental set-up is a direct implementation of the principle diagram shown in Fig. 15(a). The electrical signals driving a MZM in push-pull mode were generated at 625-Mbit/s by programming a 40-Gbit/s bit pattern generator, hence resulting in fast rise and fall times. Low pass filtering of the driving signals with a 4th order Bessel filter having a 7.5-GHz cut-off frequency was performed in order to increase their rise time to ~50 ps. In practice the proposed method will directly accommodate the rise times of lower speed signal generation electronics compatible with UWB applications. The CW laser was precisely tuned to a resonance of the MRR, as shown in the optical spectra of Figs. 17(a) and 17(c). The power coupling coefficients of the through and drop couplers of the MRR were thermally tuned, and balanced monocycle pulses were obtained in both polarities, as shown in Figs. 17(b) and 17(d).

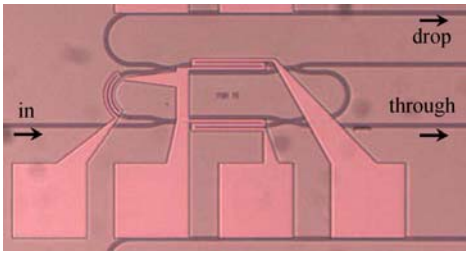

Fig. 16 Microscope picture of the fabricated coupling-tunable silicon MRR

7 Polarization diversity circuit

In all previous demonstrations, the silicon MRRs were operating on one specific polarization state since standard SOI MRRs are extremely polarization sensitive because of the high index contrast silicon waveguides. However, in a real subsystem deployed over an optical fiber link, the polarization state of the optical signal at the MRR input may change randomly over time, making standard SOI devices no longer compatible with optical processing functionalities. To realize polarization independence,

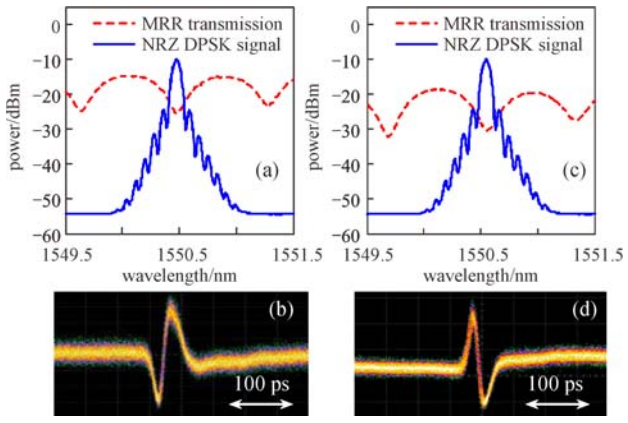

Fig. 17 Measured transfer functions at the through port of the MRR, together with the spectra of the optical NRZ-DPSK signals at 625 Mbit/s for generations of (a) negative and (c) positive polarity monocycle signals; waveform of the generated (b) negative and (d) positive polarity UWB monocycle pulse at 625 Mbit/s

polarization diversity (Pol-D) circuits based on polarization splitter and rotator (PSR) technologies are typically used [36], as shown in Fig. 18. Assuming two orthogonal polarization states (TE and TM) are present at the input of the Pol-D circuit, the first PSR_1 splits the two orthogonal polarization states into two beams of TE light. The two TE beams are then injected into the MRR, which is designed to have two identical coupling regions. With the same through transmission after the MRR, the two TE beams are combined back to two orthogonal polarization states by the second PSR_2, therefore avoiding interference. As a result, the total device exhibits a polarization independent transmission.

Figure 19(a) shows a Pol-D circuit built on the SOI platform with a single MRR and two asymmetrical directional coupler (DC)-based PSRs [37]. The asymmetrical DC-based PSR relies on the phase match between the TE and TM modes of the narrow and wide waveguides of the DC [38], as shown in the inset of Fig. 19(a). Thanks to the simple DC structure, the PSR can be fabricated by a single lithography and etching step, greatly simplifying the fabrication process of traditional multiple layer structure based PSRs [39]. Figure 19(b) shows the detailed transmission around the resonance wavelength of 1532.67 nm. Very similar Q values of 6780 and 6578 are measured for TE and TM transmissions, respectively. A remarkably low PDL less than 1 dB is demonstrated. However, the residual polarization dependence still results in a power penalty of ~4 dB at a BER of 10^{-9} between 20-Gbit/s RZ-DPSK signals demodulated with such a circuit with and without (at optimum polarization) a polarization scrambler [37].

Even though the fabrication process is simple for the asymmetrical DC-based PSR, its performance is very sensitive to the dimension of the narrow waveguide [38]. It

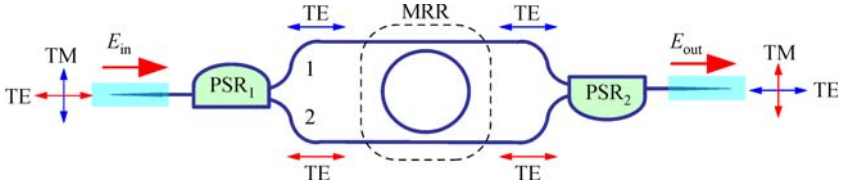

Fig. 18 Principle of a Pol-D circuit with a single MRR and two PSRs

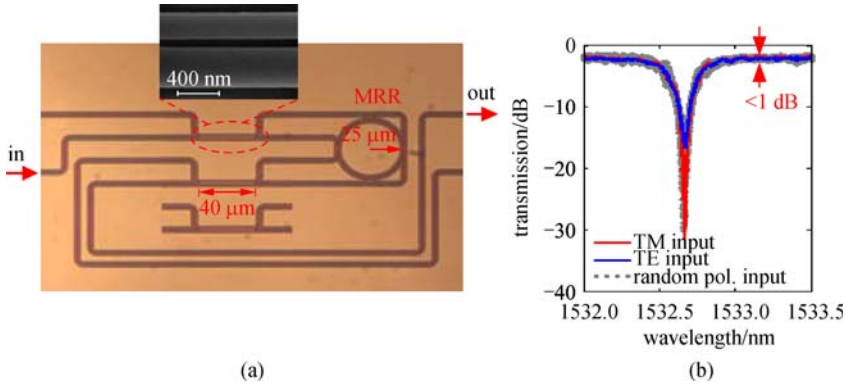

Fig. 19 (a) Microscope picture of a Pol-D circuit with a single MRR and two asymmetrical DC based PSRs. The inset shows an SEM image of the asymmetrical DC; (b) detailed transmission around the resonance wavelength of 1532.67 nm for TE, TM and 10 randomly chosen input polarization states

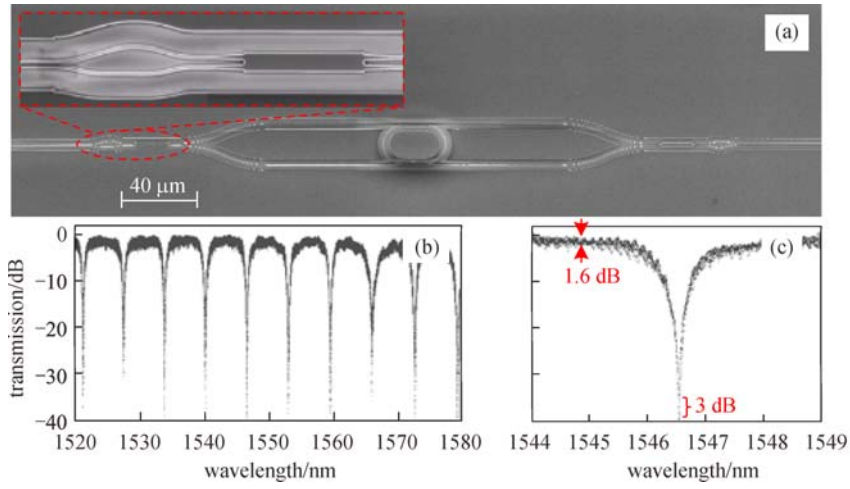

Fig. 20 (a) SEM image of a fabricated Pol-D circuit. The inset shows an SEM image of the PSR based on a tapered waveguide followed by a 2 × 2 MMI; (b) measured transmission of the Pol-D MRR over a 60-nm wavelength range and (c) details of the transmission around the resonance wavelength of 1546.52 nm for 15 randomly chosen input polarization states

is possible to increase the fabrication tolerance by introducing a taper for the wide waveguide. However, the fabrication tolerance improvement is still limited to 14 nm [40]. We have proposed and demonstrated a novel PSR based on a tapered waveguide followed by a 2 × 2 multi-mode interference (MMI) coupler [41], as shown in the inset of Fig. 20(a). It is demonstrated that the fabrication tolerance is better than 50 nm with large feature size, allowing the device to be fabricated by other fabrication methods such as deep ultraviolet (DUV) lithography. The device can also be fabricated by a simple process with one single step of lithography and ICP etching. Figure 20(a) shows a photography of the Pol-D circuit based on the novel PSR [42]. The device exhibits similar transmissions with FSR of 805 GHz and Q value of 1400 regardless of the input polarization. Figure 20(c) shows the details of the transmission around the resonance wavelength of 1546.52 nm. A lowest insertion loss of 0.5 dB is obtained. A low PDL smaller than 1.6 dB, and a high ER of 38 dB with polarization-dependent extinction ratio (PDER) better than 3 dB are measured. The fabricated Pol-D circuit was then used for NRZ-DPSK demodulation at 40 Gbit/s [42]. Figure 21(a) shows BER measurements performed for the signals demodulated by the Pol-D MRR without and with polarization scrambling at its input. The corresponding eye-diagrams are shown in Figs. 21(b) and 21(c), respectively. One can see that clear and open eye-diagrams are obtained in both cases. A power penalty of 3 dB at a BER of 10^{-9} is found between the signals demodulated with and without (at optimum polarization) the polarization scrambler, which is induced by the residual PDL and PDER. In contrast, using a standard MRR design would result in a completely closed eye diagram when polarization scrambling of the DPSK signal is performed before the resonator, as shown in Fig. 21(d).

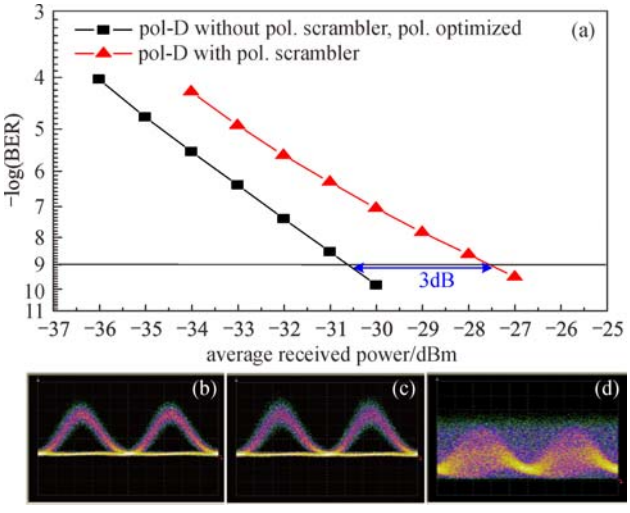

Fig. 21 (a) BER measurements for the AMI signal demodulated by the Pol-D MRR with and without the polarization scrambler; eye-diagrams of the demo-dulated AMI signals (b) without and (c) with polarization scrambler, as well as (d) the signal demodulated by a standard MRR with polarization scrambling

8 Conclusion

We have demonstrated a wide range of applications of all-optical linear signal processing using silicon MRRs. We have reviewed our recent work dealing with modulation format conversion, DPSK demodulation, modulation speed enhancement of a DML, and UWB monocycle pulse generation using silicon MRRs as passive filters. We have also described our work on improving the polarization dependence of SOI MRR devices by using Pol-D circuits with novel PSRs. As cost-effective ultra-compact passive devices, silicon MRRs may find applications for

linear signal processing in telecommunication, data-communications as well as optical interconnection systems.

References

1. Hirano M, Nakanishi T, Okuno T, Onishi M. Silica-based highly nonlinear fibers and their application. IEEE Journal of Selected Topics in Quantum Electronics, 2009, 15(1): 103–113
2. Oxenlowe L K, Ji H, Galili M, Pu M, Hu H, Mulvad H C H, Yvind K, Hvam J M, Clausen A T, Jeppesen P. Silicon photonics for signal processing of Tbit/s serial data signals. IEEE Journal of Selected Topics in Quantum Electronics, 2012, 18(2): 996–1005
3. Pelusi M D, Ta'eed V G, Fu L, Magi E, Lamont M R E, Madden S, Choi D Y, Bulla D A P, Luther-Davies B, Eggleton B J. Applications of highly-nonlinear chalcogenide glass devices tailored for high-speed all-optical signal processing. IEEE Journal of Selected Topics in Quantum Electronics, 2008, 14(3): 529–539
4. Stubkjaer K E. Semiconductor optical amplifier-based all-optical gates for high-speed optical processing. IEEE Journal of Selected Topics in Quantum Electronics, 2000, 6(6): 1428–1435
5. Langrock C, Kumar S, McGeehan J E, Willner A E, Fejer M M. All-optical signal processing using $\chi^{(2)}$ nonlinearities in guided-wave devices. Journal of Lightwave Technology, 2006, 24(7): 2579–2592
6. Bogaerts W, De Heyn P, Van Vaerenbergh T, De Vos K, Kumar Selvaraja S, Claes T, Dumon P, Bienstman P, Van Thourhout D, Baets R. Silicon microring resonators. Laser & Photonics Reviews, 2012, 6(1): 47–73
7. Marcatili E A J. Bends in optical dielectric waveguides. Bell System Technical Journal, 1969, 48(7): 2103–2132
8. Little B E, Chu S T, Haus H A, Foresi J, Laine J P. Microring resonator channel dropping filters. Journal of Lightwave Technology, 1997, 15(6): 998–1005
9. Krauss T, Laybourn P J R, Roberts J. CW operation of semiconductor ring lasers. Electronics Letters, 1990, 26(25): 2095–2097
10. Xu Q, Schmidt B, Pradhan S, Lipson M. Micrometre-scale silicon electro-optic modulator. Nature, 2005, 435(7040): 325–327
11. Hill M T, Dorren H J S, De Vries T, Leijtens X J M, Den Besten J H, Smalbrugge B, Oei Y S, Binsma H, Khoe G D, Smit M K. A fast low-power optical memory based on coupled micro-ring lasers. Nature, 2004, 432(7014): 206–209
12. Ding Y, Zhang X B, Zhang X L, Huang D. Proposal for loadable and erasable optical memory unit based on dual active microring optical integrators. Optics Communications, 2008, 281(21): 5315–5321
13. Ding Y, Zhang X, Zhang X, Huang D. Active microring optical integrator associated with electroabsorption modulators for high speed low light power loadable and erasable optical memory unit. Optics Express, 2009, 17(15): 12835–12848
14. Ding Y, Pu M, Liu L, Xu J, Peucheret C, Zhang X, Huang D, Ou H. Bandwidth and wavelength-tunable optical bandpass filter based on silicon microring-MZI structure. Optics Express, 2011, 19(7): 6462–6470
15. Yariv A. Universal relations for coupling of optical power between microresonators and dielectric waveguides. Electronics Letters, 2000, 36(4): 321–322
16. Amarnath K. Active microring and microdisk optical resonator on indium phosphide. Dissertation for the Doctoral degree. College Park: University of Maryland, 2006
17. Yu Y, Zhang X L, Huang D X, Li L J, Fu W. 20-Gb/s all-optical format conversions from RZ signals with different duty cycles to NRZ signals. IEEE Photonics Technology Letters, 2007, 19(14): 1027–1029
18. Zhang Y, Xu E, Huang D, Zhang X. All-optical format conversion from RZ to NRZ utilizing microfiber resonator. IEEE Photonics Technology Letters, 2009, 21(17): 1202–1204
19. Ding Y, Peucheret C, Pu M, Zsigri B, Seoane J, Liu L, Xu J, Ou H, Zhang X, Huang D. Multi-channel WDM RZ-to-NRZ format conversion at 50 Gbit/s based on single silicon microring resonator. Optics Express, 2010, 18(20): 21121–21130
20. Xiong M, Ozolins O, Ding Y, Huang B, An Y, Ou H, Peucheret C, Zhang X. Simultaneous RZ-OOK to NRZ-OOK and RZ-DPSK to NRZ-DPSK format conversion in a silicon microring resonator. Optics Express, 2012, 20(25): 27263–27272
21. Hansen Mulvad H C, Oxenløwe L K, Galili M, Clausen A T, Grüner-Nielsen L, Jeppesen P. 1.28 Tbit/s single-polarisation serial OOK optical data generation and demultiplexing. Electronics Letters, 2009, 45(5): 280–281
22. Hayee M I, Willner A E. NRZ versus RZ in 10–40-Gb/s dispersion-managed WDM transmission systems. IEEE Photonics Technology Letters, 1999, 11(8): 991–993
23. Ding Y, Hu H, Galili M, Xu J, Liu L, Pu M, Mulvad H C H, Oxenløwe L K, Peucheret C, Jeppesen P, Zhang X, Huang D, Ou H. Generation of a 640 Gbit/s NRZ OTDM signal using a silicon microring resonator. Optics Express, 2011, 19(7): 6471–6477
24. Hansen Mulvad H C, Galili M, Oxenløwe L K, Hu H, Clausen A T, Jensen J B, Peucheret C, Jeppesen P. Demonstration of 5.1 Tbit/s data capacity on a single-wavelength channel. Optics Express, 2010, 18(2): 1438–1443
25. Gnauck A H, Winzer P J. Optical phase-shift-keyed transmission. Journal of Lightwave Technology, 2005, 23(1): 115–130
26. Kaminow I P. Balanced optical discriminator. Applied Optics, 1964, 3(4): 507–510
27. Zhang L, Yang J Y, Song M, Li Y, Zhang B, Beausoleil R G, Willner A E. Microring-based modulation and demodulation of DPSK signal. Optics Express, 2007, 15(18): 11564–11569
28. Xu L, Li C, Wong C, Tsang H K. Optical differential-phase shift-keying demodulation using a silicon microring resonator. IEEE Photonics Technology Letters, 2009, 21(5): 295–297
29. Ding Y, Xu J, Peucheret C, Pu M, Liu L, Seoane J, Ou H, Zhang X, Huang D. Multi-channel 40 Gb/s NRZ-DPSK demodulation using a single silicon microring resonator. Journal of Lightwave Technology, 2011, 29(5): 677–684
30. Matsui Y, Mahgerefteh D, Zheng X, Liao C, Fan Z F, McCallion K, Tayebati P. Chirp-managed directly modulated laser (CML). IEEE Photonics Technology Letters, 2006, 18(2): 385–387
31. An Y, Lorences Riesgo A, Seoane J, Ding Y, Ou H, Peucheret C. Transmission property of directly modulated signals enhanced by a

micro-ring resonator. In: Proceedings of OptoElectronics and Communications Conference, OECC'2012. Busan, Korea, 2012, paper 6F3–3
32. An Y, Müller M, Estaran J, Spiga S, Da Ros F, Peucheret C, Amann M C. Signal quality enhancement of directly-modulated VCSELs using a micro-ring resonator transfer function. In: Proceedings of OptoElectronics and Communications Conference/Photonics in Switching, OECC/PS'2013. Kyoto, Japan, 2013, paper ThK3–3
33. Yao J, Zeng F, Wang Q. Photonic generation of ultrawideband signals. Journal of Lightwave Technology, 2007, 25(11): 3219–3235
34. Liu F, Wang T, Zhang Z, Qiu M, Su Y. On-chip photonic generation of ultrawideband monocycle pulses. Electronics Letters, 2009, 45 (24): 1247–1249
35. Ding Y, Huang B, Peucheret C, Xu J, Ou H, Zhang X, Huang D. Ultra-wide band signal generation using a coupling-tunable silicon microring resonator. Optics Express, 2014, 22(5): 6078–6085
36. Barwicz T, Watts M R, Popovic M, Rakich P T, Socci L, Kartner F X, Ippen E P, Smith H I. Polarization-transparent microphotonic devices in the strong confinement limit. Nature Photonics, 2007, 1 (1): 57–60
37. Ding Y, Liu L, Peucheret C, Xu J, Ou H, Yvind K, Zhang X, Huang D. Towards polarization diversity on the SOI platform with simple fabrication process. IEEE Photonics Technology Letters, 2011, 23 (23): 1808–1810
38. Liu L, Ding Y, Yvind K, Hvam J M. Silicon-on-insulator polarization splitting and rotating device for polarization diversity circuits. Optics Express, 2011, 19(13): 12646–12651
39. Zhang J, Yu M, Lo G Q, Kwong D L. Silicon-waveguide-based mode evolution polarization rotator. IEEE Journal of Selected Topics in Quantum Electronics, 2010, 16(1): 53–60
40. Ding Y, Liu L, Peucheret C, Ou H. Fabrication tolerant polarization splitter and rotator based on a tapered directional coupler. Optics Express, 2012, 20(18): 20021–20027
41. Ding Y, Ou H, Peucheret C. Wideband polarization splitter and rotator with large fabrication tolerance and simple fabrication process. Optics Letters, 2013, 38(8): 1227–1229
42. Ding Y, Huang B, Ou H, Da Ros F, Peucheret C. Polarization diversity DPSK demodulator on the silicon-on-insulator platform with simple fabrication. Optics Express, 2013, 21(6): 7828–7834

Yunhong Ding received the B.Sc. degree at College of Optoelectronic Science and Engineering, Huazhong University of Science and Technology (HUST), China, in 2006, as well as the Ph.D. degree from this same university in 2011. His Ph.D. project dealt with micro-ring resonators for lossless all-optical buffers. He was a guest Ph.D. student at the Technical University of Denmark between 2009 and 2011, where he was involved in the fabrication, characterization and system tests of silicon micro-ring resonators. His broad expertise ranges from components design and fabrication to high-speed system demonstrations using those devices.

He is currently a postdoctoral fellow at the Technical University of Denmark, working on silicon integrated devices for linear signal processing and space division multiplexing.

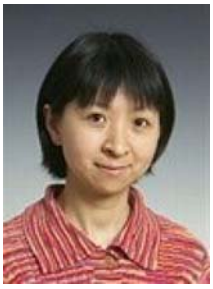

Haiyan Ou received the M.Sc. degree in semiconductor devices and microelectronics with minor in industrial enterprise management in Department of Solid State Electronics, Huazhong University of Science and Technology (HUST), Wuhan, Hubei, China, in 1997, and the Ph.D. degree in optical communication in the Institute of Semiconductors, Chinese Academy of Sciences (CAS), Beijing, China, in 2000.

She has been with the Department of Photonics Engineering, Technical University of Denmark (DTU Fotonik), Lyngby, Denmark, since 2000, first as an Assistant Professor and currently an Associate Professor. Her research interests are LEDs, fiber optics, integrated optics, nano-materials, and energy-efficient devices.

Jing Xu received the Ph.D. degree from Wuhan National Laboratory for Optoelectronics, Huazhong University of Science and Technology,Wuhan, China, in 2009.

She is currently a Postdoctoral Researcher with DTU Fotonik, Department of Photonics Engineering, Technical University of Denmark, Lyngby, Denmark. Her current research interests include high-speed optical signal processing and high-speed optical time-division multiplexing systems.

Meng Xiong received the B.Sc. degree at College of Optoelectronic Science and Engineering, Huazhong University of Science and Technology (HUST), China, in 2008. She is currently working toward the Ph.D. degree at Wuhan National Laboratory for Optoelectronics, and School of Optical and Electronic Information, HUST.

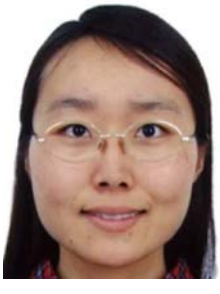

Yi An received the B.Eng. degree from Beijing University of Technology, China and the M.Sc. and Ph.D. degrees from the Technical University of Denmark (DTU). At DTU she has been involved in research activities on physical-layer functionalities for reliable optical networks, including avionic networks.

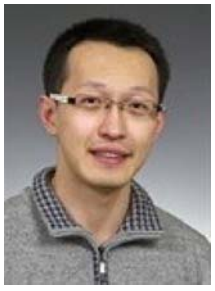

Hao Hu received the Ph.D. degree in optical communications from Tianjin University, Tianjin, China, in 2009. From 2007 to 2008, he was a Visiting Scientist at Fraunhofer Institute for Telecommunications, Heinrich-Hertz-Institute (HHI), Berlin, Germany. He is currently a Postdoctoral Researcher at the Department of Photonics Engineering, Technical University of Denmark, Lyngby, Denmark. His current research interests include Terabit Ethernet and ultrahigh-speed optical signal processing and transmission at 640 Gb/s and beyond. He is the author and coauthor of more than 60 peer reviewed publications.

Michael Galili received the Master of Science in engineering in applied physics with main focus on optics and semiconductor physics, from the Technical University of Denmark (DTU), Lyngby, Denmark, in 2003 and the Ph.D. degree in optical communications and signal processing from the Communication, Optics and Materials Department at DTU, in 2007. His Ph.D. thesis focused on optical signal processing of high-speed optical data signals.

He is currently an Associate Professor at the Department of Photonics Engineering, DTU. His current research interests include optical signal processing in various materials and platforms as well as ultra-high speed optical communications. He is the first author or coauthor of more than 80 peer reviewed scientific publications and he is educating both Master's and Ph.D. students.

Abel Lorences Riesgo received the M.Sc. degree in telecommunication engineering from the University of Oviedo in Spain, in 2010. In 2010, he worked at the Technical University of Denmark, Department of Photonics Engineering (DTU Fotonik) as a research assistant. He is currently working toward the Ph.D. degree at the Photonics Laboratory, Department of Microtechnology and Nanoscience (MC2), Chalmers University of Technology. His research is focused on phase sensitive fiber parametric amplification.

Jorge Seoane received the Telecommunication Engineer degree from the Faculty of Engineering, Bilbao, Spain, and the Ph.D. degree in optical communication from DTU Fotonik, Technical University of Denmark, Lyngby, Denmark. His work in the optical field includes contributions to migration scenarios from 10 to 40 Gbit/s in WDM systems, 100-G Ethernet systems, optical label switching and advanced modulation formats applied to both WDM and OTDM systems.

His current research interests include all-optical signal processing, advanced modulation formats, and novel methods for their amplification.

Kresten Yvind received the M.Sc.E., and Ph.D. degrees from the Research Center for Communication, Optics and Materials (COM), Technical University of Denmark (DTU), Lyngby, Denmark, in 1999 and 2003, respectively.

He is currently an Associate Professor and a Group Leader for Nanophotonic Devices at DTU Fotonik. His research interests include a broad range of topics from design, cleanroom fabrication, and testing of optical devices in InP, GaAs, and silicon.

Leif Katsuo Oxenløwe received the B.Sc. degree in physics and astronomy from Niels Bohr Institute, University of Copenhagen, Copenhagen, Denmark, in 1996, the International Diploma of Imperial College of Science, Technology, and Medicine, London, UK, in 1998, the M.Sc. degree from the University of Copenhagen, Copenhagen, Denmark, in 1998, and the Ph.D. degree from the Technical University of Denmark, Kongens Lyngby, Denmark, in 2002.

Since 2007, he has been the Group Leader of the High-Speed Optical Communications Group and since December 2009, he has been a Professor of Photonic Communications, at DTU. He is author and coauthor of more than 150 peer reviewed publications. His research interests include the field of ultra-high speed serial optical communications and optical signal processing.

Dr. Oxenløwe is the recipient of a European Research Council project (SOCRATES) dealing with the connection between ultra-high-speed serial data and Ethernet networks. He is also heading the Danish national research council project NOSFERATU and is involved in several other national and international projects.

Xinliang Zhang received the Ph.D. degree from Huazhong University of Science and Technology (HUST), Wuhan, China, in 2001. He is currently a Professor with Wuhan National Laboratory for Optoelectronics and Institute of Optoelectronics Science and Engineering, Huazhong University of Science and Technology, Wuhan, Hubei, China.

His current research interests are all-optical signal processing and related components. He has authored or coauthored 50 related papers in international journals or conferences proceedings.

Dexiu Huang graduated from the Department of Radio Engineering, Huazhong Institute of Technology (now Huazhong University of Science and Technology), Wuhan, China, in 1963.

Since then, he has been with the same university as Assistant Professor, Lecturer, Associate Professor, and Professor in 1963, 1978, 1986, and 1990, respectively. Prior to 1972, he was engaged in research on semiconductor devices and passive devices in radio engineering. From 1972 to 1981, he performed research on solid-state lasers and applications. From 1981 to 1983, he was a Visiting Scientist with the Oregon Graduate Center, focusing on semiconductor optoelectronic devices. Since then, he has been in the field of optical communication performing research on semiconductor optoelectronics devices and some passive devices. He is currently a Professor at the College of Information Science and Engineering. He is the author of five books and has authored or coauthored more than 200 papers.

Christophe Peucheret received the graduate engineering degree from Ecole Nationale Supérieure des Télécommunications de Bretagne, Brest, France, the M.Sc. degree in microwaves and optoelectronics from University College London, UK, and the Ph.D. degree from the Technical University of Denmark.

His current research interests cover all-optical signal processing, especially using parametric processes in optical fibers or other nonlinear media, space division multiplexing systems and applications of micro-ring resonators and nanophotonic devices for optical communications.